Inorganic Chemistry

Communication

pubs.acs.org/IC

Terbium(III), Europium(III), and Mixed Terbium(III)−Europium(III) Mucicate Frameworks: Hydrophilicity and Stoichiometry-Dependent Color Tunability

Sudip Mohapatra, Sangita Adhikari, Hiranya Riju, and Tapas Kumar Maji*

Molecular Materials Laboratory, Chemistry and Physics of Materials Unit, Jawaharlal Nehru Centre for Advanced Scientific Research, Jakkur, Bangalore 560 064, India

Supporting Information

ABSTRACT: Two 3D porous terbium(III) mucicate frameworks, $\{[Tb_2(Mu^{2-})_3(H_2O)_2]\cdot 4H_2O\}_n$ (**1**) and $\{[Tb(Mu^{2-})(Ox^{2-})_{0.5}(H_2O)]\cdot H_2O\}_n$ (**2**), have been synthesized under hydrothermal conditions by changing the pH of the reaction medium. Isostructural europium(III) and seven mixed terbium(III)−europium(III) mucicates were synthesized by doping different percentages of Eu^{III} under similar reaction conditions and unveiling different emission colors ranging from green to red under the same wavelength. Both dehydrated Tb^{III} metal−organic frameworks exhibit selective H_2O vapor sorption over other solvent molecules (MeOH, MeCN, and EtOH) of less polarity and bigger size and have been correlated to the highly hydrophilic pore surfaces decorated with −OH groups and O atoms from the carboxyl groups of mucicate.

Metal−organic frameworks (MOFs) with open structure have attracted considerable interest because of their promising applications in gas storage, catalysis, sensing, magnetism, and luminescence.[1] The majority of the research on MOFs has been focused on the transition-metal ions.[1a−c,g,h] Recently, lanthanides (Ln^{III}) containing MOFs have attracted substantial interest because of their structural versatility (based on different coordination numbers) with interesting photoluminescence, magnetic, and electronic properties resulting from the 4f electronic shell.[1d,e,2] In general, (Eu^{III}, Pr^{III}, Sm^{III}), (Tb^{III}, Er^{III}), and (Tm^{III}, Ce^{III}) Ln ions show red, green, and blue emission, respectively, and multiple emission colors can be achieved by adjusting the relative amounts of red, green, and blue components in a host Ln compound.[3] Moreover, materials emitting multiple colors under single-wavelength excitation are of paramount importance in the field of light display, lasers, and optoelectronic devices. The emsisson properties of the different individual Ln compounds are well documentend;[1d,e,2a] however, color modulation in Ln-based MOFs by varying the dopant concentration is yet to be properly explored.[3a,d,f] Furthermore, to date, a few lanthanide−organic frameworks with porous functionalities have been reported.[1i,2b,c] Among the different organic linkers, 2,3,4,5-tetrahydroxyhexanedioic acid (mucic acid) is a rarely used naturally occurring organic linker, and on the basis of four hydroxy and two carboxy groups, it can provide pH-dependent flexible binding modes.[4] Moreover, a long alkyl chain with four hydroxy groups can be useful for generating a flexible and porous structure. A systematic study on the effect of the pH on the framework structure[5] and the overall network topology in a metal mucicate system is yet to be reported. In this contribution, we have used mucic acid as an organic linker for the synthesis of Ln (Tb^{III} and Eu^{III})-based frameworks having a flexible coordination geometry. We have isolated two terbium(III) mucicate frameworks, $\{[Tb_2(Mu^{2-})_3(H_2O)_2]\cdot 4H_2O\}_n$ (**1**) and $\{[Tb(Mu^{2-})(Ox^{2-})_{0.5}(H_2O)]\cdot H_2O\}_n$ (**2**), by changing the pH of the reaction medium (Scheme 1). At pH ≈ 2, mucic acid acts as both a ligand and a precursor of oxalate, whereas at pH ≈ 4, it acts as a linker only. The europium(III) mucicate $\{[Eu_2(Mu^{2-})_3(H_2O)_2]\cdot 4H_2O\}_n$ (**3**) framework and a series of Eu^{III}-doped frameworks (with different atom %), isomorphs of **1**, have been synthesized, and luminescence colors of the compounds $\{[Tb_{2-2x}Eu_{2x}(Mu^{2-})_3(H_2O)_2]\cdot 4H_2O\}_n$ were easily tuned from green, green-yellow, yellow, orange, and red-orange by changing the doping concentration of the Eu^{III} ion. To the best of our knowledge, this is the first report of the color tunability and pH-controlled synthesis of lanthanide mucicate frameworks.

Scheme 1. Representing a pH-Controlled Synthesis of Terbium(III) Mucicate (1) and Terbium(III) Mucicate−Oxalate (2) Frameworks

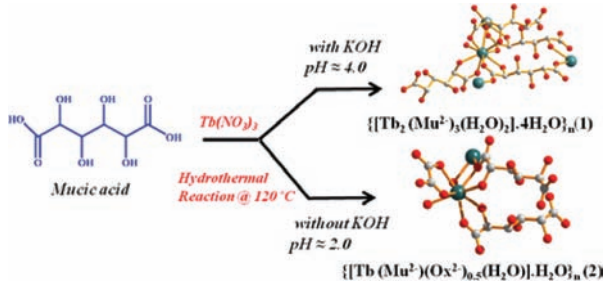

The terbium(III) mucicate frameworks have been synthesized hydrothermally at 120 °C at pH ≈ 4.0 (for **1**) and 2.0 (for **2**), see the Supporting Information (SI). Various coordination modes of mucicate (Mu^{2-}) to Tb^{III} are shown in Figure S1 in the SI. **1** and **2** crystallize in triclinic space group $P\bar{1}$ (Table S1 in the SI), and the structure determination of both **1** and **2** reveals a 3D coordination framework of Tb^{III} bridged by Mu^{2-}

Received: February 1, 2012
Published: April 18, 2012

(dianionic form of mucic acid) in **1** and Mu^{2-} and oxalate (Ox^{2-}) in **2**. There are four different types of binding modes of Mu^{2-}, viz., Mu^{2-}_a, Mu^{2-}_b, Mu^{2-}_c, and Mu^{2-}_d in compounds **1** and **2** (Figures S1 and S2 in the SI). In **1**, a nine-coordinated Tb1 center is connected to three different Mu^{2-} (Mu^{2-}_a, Mu^{2-}_b, and Mu^{2-}_c) to satisfy coordination number 8, whereas in **2**, the Tb1 center is coordinated to two Mu^{2-} (Mu^{2-}_b and Mu^{2-}_d) and one Ox^{2-} to satisfy coordination number 7 (Figure S2 in the SI). Ninth and eighth coordination of Tb1 in **1** and **2** are occupied by H_2O molecules, respectively. In **1**, Mu^{2-}_a and Mu^{2-}_b are chelated to a Tb^{III} center in tridentate (O5, O7, and O8) and bidentate (O9 and O11) fashion, respectively, to build a 1D zigzag chain along the crystallographic *c* direction (Figure S3a in the SI). The chains are lying on the *ac* plane (Figure S3b in the SI), which are diagonally pillared by Mu^{2-}_c, where syn−anti-bridged carboxylate O atoms (O1 and O2) and O3 from OH coordinated to Tb^{III} centers result in a 3D structure (Figure 1a). In compound **2**, each eight-coordinated Tb1 center is

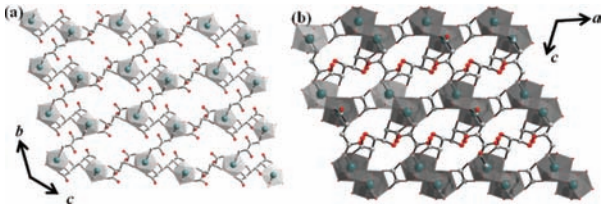

Figure 1. (a) 3D structure of **1** viewed along the *a* axis formed by the three different bindings of Mu^{2-} (b) 3D structure of **2** viewed along the *b* axis formed by the two different Mu^{2-} and one Ox^{2-}.

chelated to Ox^{2-} through the O atoms (O3 and O7) and to two Mu^{2-} (Mu^{2-}_b and Mu^{2-}_d) through O atoms (O1, O2, and μ_2-O4, O8). A 2D sheet is formed by coordination of Mu^{2-}_b and Mu^{2-}_d in the crystallographic *bc* plane (Figure S4 in the SI), which is further connected by Ox^{2-} along the crystallographic *a* direction to form a 3D coordination framework (Figure 1b). Topological analysis suggests that both frameworks have a 7-c uninodal structure with point symbol $\{3^6;4^8;5^6;6\}$ and the type of topology is svi-x/*I*4/*mcm* → *Ibam*. Bond sets: 1, 4, 5, 6: svi-x; obtained from the TOPOS Topological Database (TTD)[6b] (Figure S5 in the SI). Tb1−O bond distances are in the range of 2.315(5)−2.574(4) Å and 2.288(8)−2.444(4) Å for **1** and **2**, respectively (Tables S2 and S3 in the SI). The 3D framework of **1** contains dumbbell-shaped channels (4.9 × 6.9 $Å^2$) along the *a* axis and rectangular-shaped channels (2.8 × 1.7 $Å^2$) along the *b* axis occupied by the guest H_2O molecules (Figures S6a,b and S7a in the SI). Compound **2** contains hexagonal-shaped channels along the *c* axis with a smaller pore aperture (3.85 × 2.31 $Å^2$). (Figures S6c and S7b in the SI). Compounds **1** and **2** contain four and one guest H_2O molecules per formula unit, respectively. The effective pore dimension of the dumbbell-shaped channels in **1** is less because of the presence of hanging hydroxyl groups on the pore walls. Calculations using *PLATON*[6a] suggest that the dehydrated frameworks of **1** and **2** contain 23.7% and 17% void space to the total crystal volume.

Thermogravimetric analysis (TGA) suggests the concomitant release of both coordinated and crystalline H_2O molecules in compound **1** and the stepwise release of crystalline and coordinated H_2O molecules in compound **2** (Figure S8 in the SI). Both dehydrated frameworks (**1′** and **2′**) are stable up to 230 °C. Powder X-ray diffraction (PXRD) studies of both dehydrated frameworks show significant changes, indicating structural change after removal of the guest and Tb^{III}-bound H_2O molecules rather than collapse of the framework (Figure S9 in the SI).

To examine the permanent porosity, the dehydrated frameworks **1′** and **2′** were subjected to adsorption studies with N_2 (kinetic diameter 3.6 Å) and CO_2 (kinetic diameter 3.3 Å) at 77 and 195 K, respectively. Both isotherms show typical type II profiles with small uptake up to $P/P_0 \sim 1$, indicating only surface adsorption (Figure S10 in the SI). These results can be correlated to the smaller effective pore sizes of **1′** and **2′** compared to the kinetic diameters of N_2 and CO_2. In the case of **1′**, the effective pore size is smaller because of blocking by pendent hydroxyl groups. H_2O (kinetic diameter 2.65 Å), MeOH (4.0 Å), MeCN (4.3 Å), and EtOH (4.5 Å) vapor sorption isotherms were measured under ambient conditions to study the selectivity based on the polarity and pore size of the framework. As shown in Figure S11 in the SI, the sorption profile of H_2O shows a typical type I curve with steep uptake at the low-pressure region, whereas other solvents are not adsorbed by any of the compounds, suggesting the strong hydrophilic nature of the pore surface. The amounts of final uptake are about 160 and 40 mL g^{-1} at $P/P_0 \sim 1$, which corresponds to about 7 and 1 molecules of H_2O per formula unit of **1′** and **2′**, respectively. The values of βE_0, which reflect the adsorbate−adsorbent affinity, are significantly high (9.7 kJ mol^{-1} (**1′**) and 8.99 kJ mol^{-1} (**2′**), also suggesting the strong hydrophilic nature of the framework, which can be attributed to the presence of pendent oxygen (carboxyl group) and hydroxyl groups on the pore surface. The effective pore dimensions in **1′** and **2′** are also not sufficient for the inclusion of larger guest molecules like MeOH, MeCN, and EtOH.

The PXRD pattern of **3** is similar to that of **1**, and indexing of the pattern using the *KOHL* program[6c] suggests a cell parameter identical with that of **1** (Table S4 in the SI), confirming that **1** and **3** are isomorphous (Figure S12 in the SI). Typical emission spectra of **1** and its europium analogue **3** show their respective characteristic peaks when excited at 315 nm for both compounds. Compound **1** shows emission peaks at 485, 545, 585, and 620 nm corresponding to transitions from $^5D_4$ to ^7F_J (where J = 6−3, respectively) for Tb^{III} (Figure S13 in the SI), whereas compound **3** exhibits emission peaks at 590, 615, 650, and 693 nm related to $^5D_0$-to-^7F_J transitions, where J = 1−4, respectively (Figure S14 in the SI). The red emission of the pure Eu^{III} compound (**3**) is due to the most intense peak at 615 nm for a $^5D_0$-to-$^7F_2$ transition, and the green color of the pure Tb^{III} compound is due to the most intense peak at 545 nm for a $^5D_4$-to-$^7F_5$ transition. Furthermore, Tb^{III} and Eu^{III} are a well-known donor−acceptor pair, where Tb^{III} acts as a donor and Eu^{III} acts as an acceptor, and they have green and red emission, respectively, as described previously. Eu^{III} and Tb^{III} have similar charge and ionic radii; therefore, Eu^{III} can be doped easily in the Tb^{III} compound and the corresponding emission color can be tuned based on the concentration of the acceptor Eu^{III} through an energy-transfer process. Thus, to obtain color tunability based on compound **1**, we varied the doping amount of Eu^{III} in **1** and isolated seven mixed Tb^{III}−Eu^{III} compounds of Eu^{III} contents of 50, 24, 15, 7, 4, 1.24, and 0.6 atom %. The compositions of the compounds were confirmed by energy-dispersive X-ray analysis. The PXRD patterns of all mixed Tb^{III}−Eu^{III} compounds are similar to that of compound **1**, indicating that they are all isostructural (Figure

dx.doi.org/10.1021/ic300237e | *Inorg. Chem.* 2012, 51, 4891−4893

S12 in the SI). By increasing the Eu^{III} content in the system, we observed that the emission color changes from green to red gradually (inset of Figure 2). As we know, the Ln ion possesses

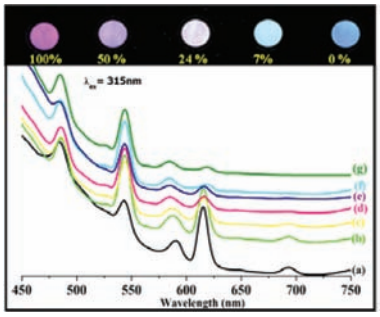

Figure 2. (Top) Color of different samples of different Eu^{III} contents in **1** under UV light. (Bottom) Emission spectra of mixed Tb^{III}–Eu^{III} compounds with different percentages of Eu doping (λ_{ex} = 315 nm): (a) 50%; (b) 24%; (c) 15%; (d) 7%; (e) 4%; (f) 1.24%; (g) 0.6%.

a very low extinction coefficient because of the intraconfigurational f–f transition and has very weak emission when directly excited. The problem of inefficient emission can be overcome via the indirect excitation of a coordinated organic ligand, and this phenomenon is generally known as sensitization or the antenna effect. In all of the compounds, mucic acid is acting as an antenna. In order to understand the energy-transfer phenomenon, we have excited different Eu-doped Tb compounds at 315 nm. The emission spectra and decay profiles for different compounds are shown in Figures 2 and S15 in the SI. The spectra of the $Tb_{2-2x}Eu_{2x}$ compounds show peaks at 485, 545, 589, and 615 nm; among them, the most intense peaks are at 545 and 615 nm for green and red emission, respectively. The intensities of the peaks at 545 and 615 nm decrease and increase, respectively, with increasing percentage of Eu^{III} in $\{[Tb_{2-2x}Eu_{2x}(Mu^{2-})_3(H_2O)_2]\cdot 4H_2O\}_n$. The lifetimes of the $^5D_0$ (Eu^{III}) and $^5D_4$ (Tb^{III}) states increase and decrease in the doped sample from the pure compound, implying the presence of Förster resonance energy transfer (FRET) from Tb^{III} to Eu^{III} (SI).[3I,j] The efficiency of energy transfer within a single donor–acceptor pair at distance r is $E = R_0^6/(R_0^6 + r^6)$, where R_0 is the Förster distance. Because of the longer distance (6 Å) between the Tb^{III} and Eu^{III} centers, FRET would be weak in doped compounds, with a very low concentration of the acceptor (Eu^{III}; Table S6 in the SI).

In conclusion, we have isolated two different terbium (III) mucicate compounds and one isostructural europium(III) mucicate compound at two different pH values and structurally characterized them. High-temperature acidic conditions produce oxalate by decomposition of the ligand. This is the first report of the synthesis of two different mucicate MOFs by varying the pH of the medium. Both the frameworks are hydrophilic in nature. Mixed lanthanide Tb_xEu_{1-x} compounds are synthesized by doping different percentages of Eu^{III} into framework **1**, and composition-dependent emission color and energy-transfer efficiency have been demonstrated. We are trying to explore the magnetic and sensing properties of these compounds, which will be published later.

■ ASSOCIATED CONTENT

Ⓢ Supporting Information

X-ray crystallographic details in CIF format, detailed experimental procedures, excitation and emission spectra, PXRD patterns, and TGA profiles. This material is available free of charge via the Internet at http://pubs.acs.org.

■ AUTHOR INFORMATION

Corresponding Author

*E-mail: tmaji@jncasr.ac.in.

Notes

The authors declare no competing financial interest.

■ ACKNOWLEDGMENTS

S.M. thanks the CSIR, Government of India, for a fellowship. S.A. and H.R. thank the JNCASR for the Summer Research Fellowship Programme. The authors thank Dr. R. Viswanatha and G. K. Murthi (JNCASR) for help with lifetime measurements.

■ REFERENCES

(1) (a) An, J.; Farha, O. K.; Hupp, J. T.; Pohl, E.; Yeh, J. I.; Rosi, N. L. *Nat. Commun.* **2012**, *3*, 604. (b) Czaja, A. U.; Trukhan, N.; Muller, U. *Chem. Soc. Rev.* **2009**, *38*, 1284. (c) Kitagawa, S.; Kitaura, R.; Noro, S.-i. *Angew. Chem., Int., Ed.* **2004**, *43*, 2334. (d) Allendorf, M. D.; Bauer, C. A.; Bhakta, R. K.; Houk, R. J. T. *Chem. Soc. Rev.* **2009**, *38*, 1330. (e) Cui, Y.; Yue, Y.; Qian, G.; Chen, B. *Chem. Rev.* **2012**, *112* (2), 1126. (f) Kurmoo, M. *Chem. Soc. Rev.* **2009**, *38*, 1353. (g) Suh, M. P.; Park, H. J.; Prasad, T. K.; Lim, D.-W. *Chem. Rev.* **2012**, *112* (2), 782. (h) Hazra, A.; Kanoo, P.; Maji, T. K. *Chem. Commun.* **2011**, *47*, 538. (i) Mohapatra, S.; Hembram, K. P. S. S.; Waghmare, U.; Maji, T. K. *Chem. Mater.* **2009**, *21*, 5406. (j) Lun, D. J.; Waterhouse, G. I. N.; Telfer, S. G. *J. Am. Chem. Soc.* **2011**, *133*, 5806.

(2) (a) Sivakumar, S.; Reddy, M. L. P.; Cowley, A. H.; Butorac, R. R. *Inorg. Chem.* **2011**, *50*, 4882. (b) Lama, P.; Bharadwaj, P. K. *Cryst. Growth Des.* **2011**, *11*, 5434. (c) Gurunatha, K. L.; Mohapatra, S.; Suchetan, P. A.; Maji, T. K. *Cryst. Growth Des.* **2009**, *9*, 3844.

(3) (a) Evans, R. C.; Carlos, L. D.; Douglas, P.; Rocha, J. *J. Mater. Chem.* **2008**, *18*, 1100. (b) He, G.; Guo, D.; He, C.; Zhang, X.; Zhao, X.; Duan, C. *Angew. Chem., Int. Ed.* **2009**, *48*, 6132. (c) Li, G.; Hou, Z.; Peng, C.; Wang, W.; Cheng, Z.; Li, C.; Lian, H.; Lin, J. *Adv. Funct. Mater.* **2010**, *20*, 3446. (d) Liu, K.; You, H.; Zheng, Y.; Jia, G.; Song, Y.; Huang, Y.; Yang, M.; Jia, J.; Guo, N.; Zhang, H. *J. Mater. Chem.* **2010**, *20*, 3272. (e) Zhang, X.; Ballem, M. A.; Hu, Z.-J.; Bergman, P.; Uvdal, K. *Angew. Chem., Int. Ed.* **2011**, *50*, 5729. (f) Guo, H.; Zhu, Y.; Qiu, S.; Lercher, J. A.; Zhang, H. *Adv. Mater.* **2010**, *22*, 4190. (g) Yamase, T.; Naruke, H. *J. Phys. Chem. B* **1999**, *103*, 8850. (h) Choi, C.-L.; Yen, Y.-F.; Sung, H. H. Y.; Siu, A. W. H.; Jayarathne, S. T.; Wong, K. S.; Williams, I. D. *J. Mater. Chem.* **2011**, *21*, 8547. (I) Biju, S.; Ambili Raj, D. B.; Reddy, M. L. P.; Jayasankar, C. K.; Cowley, A. H.; Findlater, M. *J. Mater. Chem.* **2009**, *19*, 1425. (j) de Lill, D. T.; de Bettencourt-Dias, A.; Cahill, C. L. *Inorg. Chem.* **2007**, *46*, 3960.

(4) (a) Wong, K. L.; Law, G. L.; Yang, Y. Y.; Wong, W. T. *Adv. Mater.* **2006**, *18*, 1051. (b) Lakatos, A.; Bertani, R.; Kiss, T.; Venzo, A.; Casarin, M.; Benetollo, F.; Ganis, P.; Favretto, D. *Chem.—Eur. J.* **2004**, *10*, 1281. (c) Dornyei, A.; Garribba, E.; Jakusch, T.; Forgo, P.; Micera, G.; Kiss, T. *Dalton Trans.* **2004**, 1882.

(5) (a) Khan, N. A.; Jun, J. W.; Jhung, S. H. *Eur. J. Inorg. Chem.* **2010**, 1043. (b) Förster, P. M.; Burbank, A. R.; Livage, C.; Ferey, G.; Cheetham, A. K. *Chem. Commun.* **2004**, 368. (c) Förster, P. M.; Stock, N.; Cheetham, A. K. *Angew. Chem., Int. Ed.* **2005**, *44*, 7608. (d) Mahata, P.; Prabu, M.; Natarajan, S. *Inorg. Chem.* **2008**, *47*, 8451.

(6) (a) Spek, A. L. *PLATON, Molecular Geometry Program*; University of Utrecht: Utrecht, The Netherlands, 1999. (b) Balatov, V. A.; Shevchenko, A. P. *TOPOS, Program Package for multipurpose crystallochemical analysis*; Samara State University: Samara, Russia, 1989–2008. (c) Kohlbeck, F.; Hörl, E. M. *J. Appl. Cyrst.* **1976**, *9*, 28.